Synthesis, characterisation, superoxide dismutase and catalase activities of functionalised silica nanoparticles

Xiaohong Chen, Wu Jiang, Qingrong Cheng, Zhiquan Pan, Hong Zhou

Key Laboratory for Green Chemical Process of Ministry of Education, Wuhan Institute of Technology, Wuhan 430073, People's Republic of China
E-mail: hzhouh@126.com

Published in Micro & Nano Letters; Received on 7th November 2013; Accepted on 6th January 2014

Silica nanoparticles (NPs) modified by imidazole, carboxyl and phenol groups were designed and synthesised. The particles were characterised by Fourier transform infrared spectroscopy, thermogravimetric analysis techniques, scanning electron microscopy and atomic absorption spectroscopy. Studies on superoxide dismutase (SOD) and catalase-like activities of the NPs show that the NPs have both a high catalase-like activity with a 100% conversion rate of H_2O_2 and SOD activity with $IC_{50} = 0.023$ mg/ml, exhibiting the activity level of 10 U/ml biological SOD.

1. Introduction: Reactive oxygen species (ROS), such as superoxide anion, hydroxyl radical or hydrogen peroxide [1], are excessively produced in several clinical states, and their injurious effects contribute to the pathogenesis of many diseases [2]. It is well known that superoxide anions can be scavenged by the combined action of superoxide dismutase (SOD) and catalase (CAT), where SOD converts them into hydrogen peroxide, which is then transformed into oxygen and water by CAT [1]. Nanoparticles (NPs) could be an effective drug delivery system for antioxidant enzymes because of their ability to release the encapsulated therapeutic agents in intra- and extracellular compartments at a sustained rate [2]. NPs have received tremendous interest because of their unique optical properties, fascinating catalytic activities and potential applications [3]. They are now widely applied in cosmetics, electronics and medical fields [4]. In the study of the SOD/CAT mimics, it has been found that salen Mn complexes and certain metalloporphyrins are highly effective mimics having both SOD and CAT activities [5]. However, the applications of these mimics are still limited by the lack of a long-term stability as well as difficulties in recovery and recycling. Recently, how to address these problems has focused on loading the mimics on some solid support materials [6].

Silica NPs having a high density of silanol groups on the surface are potential candidates to be modified with various kinds of compounds by grafting the silanol groups with a wide range of organic functional species. The introduction of the organic groups provides a suitable support for the immobilisation of the biomolecules [7]. Sub-micron sized polymeric spheres are promising delivery systems in the pharmaceutical field. They are ideal carriers for low molecular weight drugs, oligonucleotides and peptides because they can increase the solubility of hydrophobic drugs, reduce toxicity and enhance the availability of those therapeutic agents [8]. The activity study of natural SOD shows that the structure of its active centre is the key factor to exhibit the function, whereas the active centre contains metal ions, such as Cu(II)/Zn (II), Mn(II) or Fe(II), as well as imidazole groups from histidine residue. To combine the superiority of both the NPs and the active centre structure, NPs (SiO_2/vinymethyltrimethoxysilane (VTMOS)/methacrylic acid (MAA)/NH_2/HL/Mn), consisting of a silica core and a modified surface by variations of the functional groups (shown in Fig. 1), were designed and synthesised. This mimic was proven to have both CAT and SOD enzymatic functions.

2. Materials and methods

2.1. Materials: Tetraethyl orthosilicate (TEOS, 98%), MAA, 98%, potassium persulfate (APS), 2-(4-morpholino)ethanesulfonic acid (MES), ammonia hydroxide (25%), *N*-hydroxysuccinimide (NHS), 5-methylsalicylaldehyde, paraformaldehyde, hydrobromic acid (40%), ethylenediamineanhydrous, ethylene diamine tetraacetic acid (EDTA), vitamin B2, $Na_2HPO_4{\cdot}12H_2O$ and $NaH_2PO_4{\cdot}2H_2O$, H_2O_2 (30%), purchased from the Sinopharm Chemical Reagent Co. Ltd were of analytical grade. VTMOS, 1-ethyl-(3-dimethyllaminopropyl) carbodiie hydrochlide, histidine, nitrotetrazolium blue chloride (NBT), methionine (MET) were purchased from the Alfa Aesar Company. Ethanol was purified by a general method before use. Bromomethyl-5-methylsalicylaldehyde was prepared according to the method in the literature [9].

2.2. Preparation of the mimic

2.2.1 Synthesis of the SiO_2/VTMOS template colloidal particles and carboxyl-modified NPs (SiO_2/VTMOS/MAA): *SiO_2/VTMOS:* A typical synthesis procedure was similar to that described in the literature [8]: 125 g ethanol, 13 g TEOS, 15 g ammonia and 50 g deionised water, respectively, were mixed and stirred at 30°C for 24 h. Then, an excessive amount of VTMOS (2.0 g) was added dropwise to introduce vinyl groups onto the silica particle surface under an argon atmosphere for another 24 h. Residual VTMOS was removed by washing the particles with a mixture of ethanol and water (the volume ratio was 1:1) by centrifuge. The product was then redispersed in water for further use.

SiO_2/VTMOS/MAA [10]: 100 ml of the obtained suspension (1.0 g SiO_2/VTMOS) was stirred for 30 min under an argon atmosphere to remove the oxygen inside, then a calculated amount of MAA (MAA: $SiO_2 = 3{:}1$) and APS (8% MAA) were added and stirred for another 30 min at room temperature. The mixture was stirred for 4 h at 80°C under an argon atmosphere. The resulting carboxyl-modified silica NPs were centrifuged and thoroughly washed with water to remove the unreacted monomers and the other soluble impurities.

2.2.2 Functionalisation of the SiO_2/VTMOS/MAA microspheres with the primary amine groups: *SiO_2/VTMOS/MAA/NH_2 [11]:* One gram of SiO_2/VTMOS/MAA was suspended in 60 ml of 0.1 M MES buffer and stirred for 1 h. To the above polymer solution, 30 mmol EDC and 30 mmol NHS were added. After 5 h stirring, 3 mmol (0.18 g) of ethylene diamine was added. The reaction

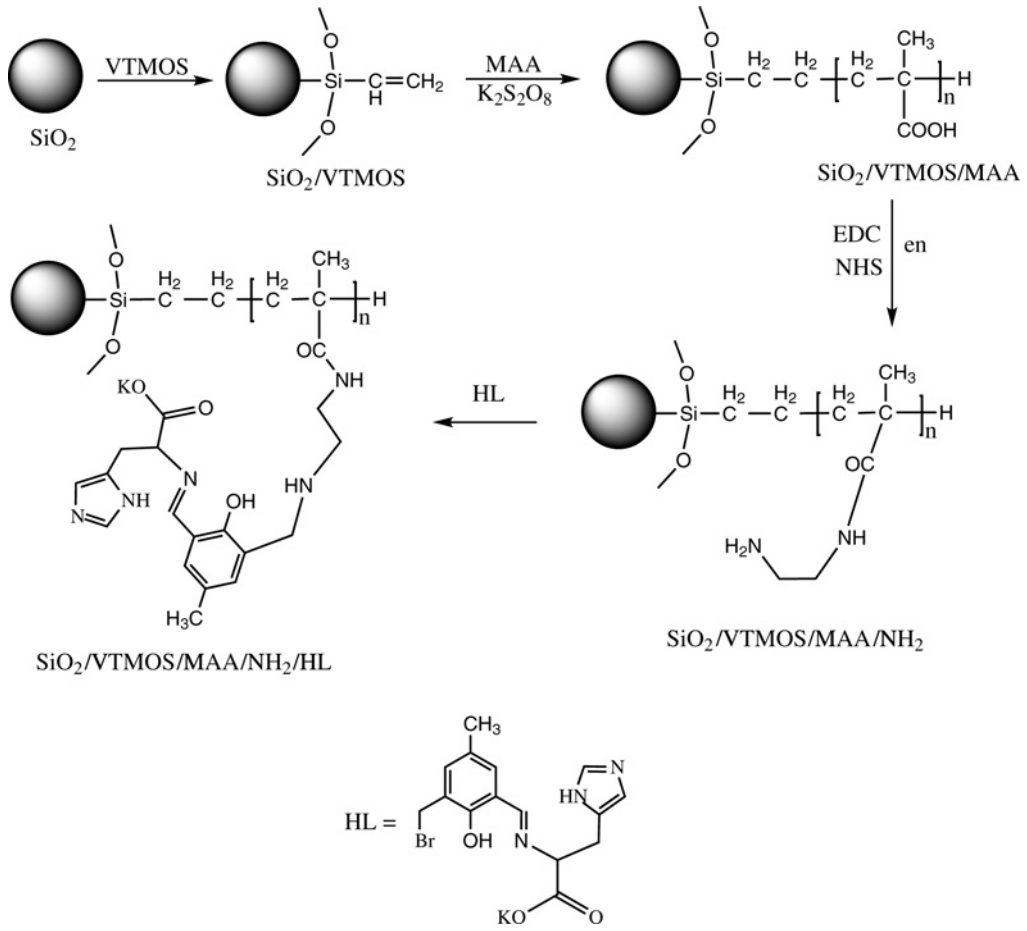

Figure 1 *Synthesis route of the NPs*

mixture was incubated overnight while stirring at 30°C. The formed particles were cleaned via repetitive centrifugation and redispersion cycles by using deionised water.

2.2.3 Synthesis of Schiff base compound Histidine: The synthesis procedure was depicted as follows [12]: bromomethyl-5-methylsalicylaldehyde (1.145 g, 5 mmol) was dissolved in 20 ml ethanol and stirred at 50°C. Then, 20 ml distilled ethanol containing histidine (0.775 g, 5 mmol) and KOH (0.28 g, 5 mmol) was added dropwise to the above solution under an argon atmosphere to give the product histidine (HL), which is the [1+1] condensation product of bromomethyl-5-methylsalicylaldehyde and histidine. The structure of HL is shown in Fig. 1.

2.2.4 Synthesis of the NPs (SiO_2/VTMOS/MAA/NH_2/HL/Mn): *SiO_2/VTMOS/MAA/NH_2/HL:* One gram of SiO_2/VTMOS/MAA/NH_2 was dispersed in 20 ml ethanol. Ten millilitres of ethanol containing 1 g HL and three drops of water were added into the dispersion liquid. An excessive amount of triethylamine was added. The resulting SiO_2/VTMOS/MAA/NH_2/HL core–shell particles were centrifuged and thoroughly washed with distilled ethanol [9].

SiO_2/VTMOS/MAA/NH_2/HL/Mn: To the 20 ml ethanol solution of 0.5 g SiO_2/VTMOS/MAA/NH_2/HL, 10 ml distilled ethanol containing 0.5 g $Mn(OAc)_2{\cdot}12H_2O$ was added dropwise. The product was purified by repetitive centrifugation and redispersion cycles using deionised water.

2.2.5 Characterisation: Fourier transform infrared spectroscopy (FTIR) spectroscopic analysis was performed on a Vector 22 FTIR spectrophotometer using KBr discs. Thermogravimetric analysis (TGA) was performed on a Q50 TGA (USA). About 20 mg of the sample was placed in a platinum crucible and the decomposition profiles of the TGA were recorded at a heating rate of 10°C/min from 10 to 800°C in a nitrogen atmosphere. Scanning electron microscopy (SEM) images were obtained using a Hitachi S4800 microscope. Mn concentration was determined by an atomic absorption spectroscopy (AAS, PinAAcle900T) spectrometer. The content of Mn in the samples was calculated from relevant calibration curves after correcting the data with blank results. Typically, 0.001 g of the catalyst sample was digested with 5 ml concentrated HNO_3 and heated to boiling. The obtained solution was then diluted to 100 ml in a volumetric flask by diluted HCl and was analysed by atomic absorption spectroscopy (AAS). The UV spectrum was tested by a Shimadzu UV-2450.

2.3. Catalysis: SOD activity of the product was tested by a modified NBT reduction assay [13, 14]. Briefly, 0.25 ml of an EDTA (1×10^{-4} M) solution was transferred into a 10 ml glass flask followed by the addition of 0.25 ml of the NP dispersion or PBS buffer solution (0.05 M, pH = 7.8), 1.25 ml of 0.01 M MET solution, 2.25 ml of 6.8×10^{-6} M V_{B2} solution and 1 ml of 9.32×10^{-5} M NBT solution, respectively. The MET, V_{B2}, NBT and EDTA solutions used above were all prepared with a PBS buffer solution. The mixture was incubated for 10 min at 37°C in the dark first and then constantly lighted for 6 min. Absorbances at 560 nm of the sample before (A'_m) and after (A_m) lighting were both measured by UV. Background absorbance was corrected by subtracting the value of the mixture without illumination.

CAT activity of the product was tested by measuring the volumetric amount of the produced dioxygen [15] in the process of H_2O_2 decomposition. The experiment was performed in a

doi: 10.1049/mnl.2013.0646

self-made saddle-type glassware, which can carry the solution and the solid sample separately and easily mix the samples together by tilting the glassware. The reactor was connected to a graduated burette filled with water and dioxygen evolution was measured at 1 min time intervals by volumometry. The amount of dioxygen was calculated from the volume of the produced oxygen gas, trapped in a burette, by using the ideal-gas equation. The initial rates observed were expressed as mol/s and were calculated from the maximum slope of the curve describing the evolution of O_2 against time [16].

3. Results and discussion

3.1. Characterisation: The infrared spectra of SiO_2/VTMOS (curve *a*), SiO_2/VTMOS/MAA (curve *b*), SiO_2/VTMOS/MAA/NH_2 (curve *c*) and SiO_2/VTMOS/MAA/NH_2/HL (curve *d*) are shown in Fig. 2. All four curves contain a peak at 1089 cm^{-1} because of the Si–O vibration, indicating that the samples include SiO_2. From the curve *a*, the peaks at 1634 and 1408 cm^{-1} are assigned to the stretching vibrations and the scissor vibration of C=C, respectively. Compared with curve *a*, the peak at 1717 cm^{-1} is observed in curve *b*, it is assigned to the stretching vibration of C=O [10] and the peaks at 1634 and 1408 cm^{-1}, respectively, in SiO_2/VTMOS/MAA are very weak, indicating that the C=C bonds in SiO_2/VTMOS have participated in the addition reaction. The peaks at 1646 and 1544 cm^{-1}, respectively, can be assigned to the stretching vibration of C=O [8] and the scissor vibration of C–N–H [8] of acylamide in SiO_2/VTMOS/MAA/NH_2 (curve *c*). Owing to the overlap of C=N and C=O, the absorption peaks in curves *c* and *d* are very similar to each other except for slight shifts.

The amount of the organic content in the modified silica NPs was quantitatively determined by the TGA, shown in Fig. 3. All the samples exhibit similar weight loss trends. The weight loss between 10 and 200°C can be attributed to the evaporation of the physically adsorbed water, and the weight loss from 200 to 600°C is related to the decomposition of the organic component in the hybrid particles and water loss from the condensation of the adjacent silanol bonds. The whole weight loss of the samples increases by increasing the feed of the organic groups to the silica core. The percentages of weight loss are listed in Table 1.

Fig. 4 shows the SEM images of SiO_2/VTMOS (Fig. 4*a*), SiO_2/VTMOS/MAA (Fig. 4*b*), SiO_2/VTMOS/MAA/NH_2 (Fig. 4*c*) and SiO_2/VTMOS/MAA/NH_2/HL (Fig. 4*d*), suggesting that the particles are spherical with average sizes of 330, 340, 350 and 380 nm, respectively. The phenomenon of the size increasing is in accordance with the step loading of the relative organic compounds on the surface of SiO_2. The bigger size difference between Figs. 4*c* and *d* is in agreement with the results of the TGA, the organic content in Fig. 4*d* is almost 3.97 times than that in Fig. 4*c*.

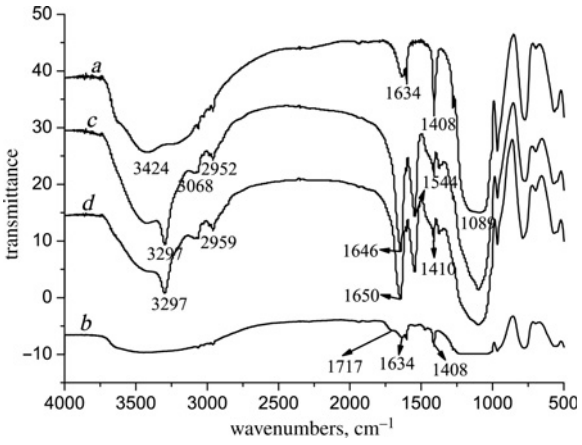

Figure 2 *IR spectra of SiO_2/VTMOS (a); SiO_2/VTMOS/MAA (b); SiO_2/VTMOS/MAA/NH_2 (c); and SiO_2/VTMOS/MAA/NH_2/HL (d)*

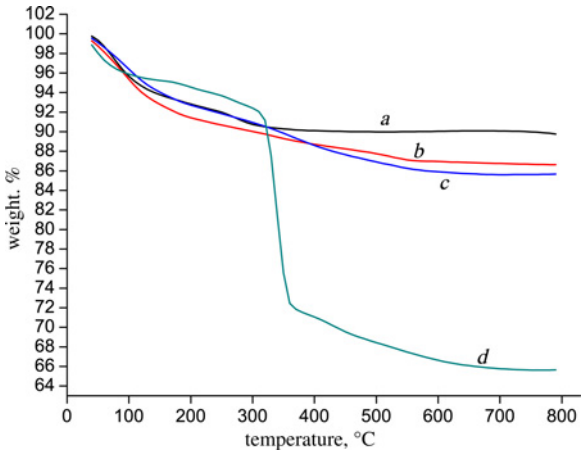

Figure 3 *TGA curves of SiO_2/VTMOS (a); SiO_2/VTMOS/MAA (b); SiO_2/VTMOS/MAA/NH_2 (c); and SiO_2/VTMOS/MAA/NH_2/HL (d)*

Table 1 Weight loss of the samples analysed by the TGA data

Sample	200–600°C, %
SiO_2/VTMOS	2.78
SiO_2/VTMOS/MAA	4.48
SiO_2/VTMOS/MAA/NH_2	6.81
SiO_2/VTMOS/MAA/NH_2/HL	27.08

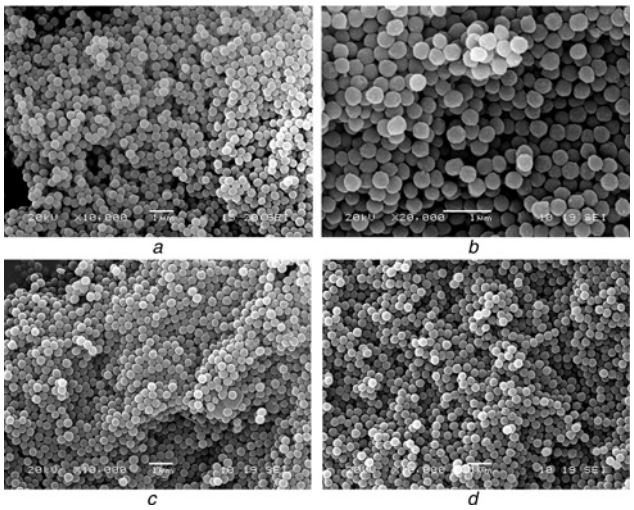

Figure 4 *SEM pictures of SiO_2/VTMOS (Fig. 4a); SiO_2/VTMOS/MAA (Fig. 4b); SiO_2/VTMOS/MAA/NH_2 (Fig. 4c); and SiO_2/VTMOS/MAA/NH_2/HL (Fig. 4d)*

The metal content of the catalyst was analysed by AAS. The Mn content in the polymer-anchored NPs, calculated from the relevant calibration curves after correcting the data with blank results, was 4.4 wt%. This content is comparable with that in the other metal-containing NPs [17]. The immobilisation of the metal ions on the NPs may be because of the availability of the muti-functional groups on the surface of the NPs.

3.2. Catalytic study: The SOD activity of the NPs has been tested: In the absence of the NPs, superoxide anions were generated by

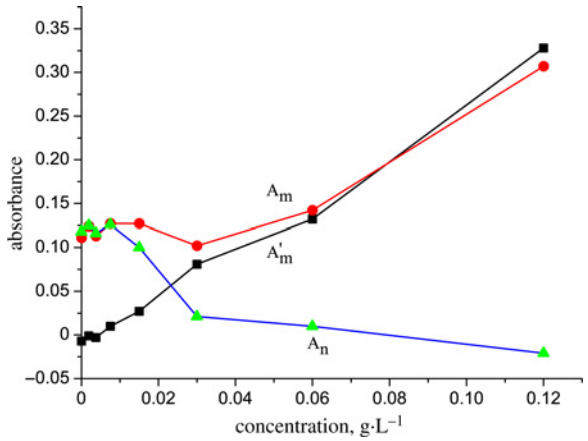

Figure 5 *Absorbance changes with the concentration of the samples*
Content of the solution: 0.25 ml EDTA (1×10^{-4} M) solution, 1.25 ml of 0.01 M MET solution, 2.25 ml of 6.8×10^{-6} M V_{B2} solution and 1.0 ml 9.32×10^{-5} M NBT solution + different mass concentration of the catalyst dispersed in a 0.25 ml PBS buffer solution

riboflavin reacting with NBT in air under lighting to yield a blue substance, methyl hydrazone, which has a maximum absorbance at 560 nm. However, in the presence of the NPs, the absorbance at 560 nm was found to be decreasing greatly with the concentration of the NPs because of the removing of the superoxide anions by the NPs.

Fig. 5 shows the absorbance changes with the concentration of the samples before (A'_m) and after (A_m) lighting. The absorbance values of the two curves exhibit the same trend, increasing with the concentration of the NPs. This trend contributed to the absorption of the sample, the higher the concentration and the stronger the absorbance. When the concentration of the NPs is zero, the difference A_m–A'_m (set as A_n) is maximal, illustrating that a blue substance has formed under illumination. A_n decreases with the increase of the concentration of the NPs. This can be ascribed to the diminishing of the blue substance in the system because of the superoxide anions being disproportionated by the NPs. Fig. 6 shows the inhibition of the blue methyl hydrazone formation changes with the NP concentration. The chromophore concentration required to yield a 50% inhibition of the reduction of NBT (IC_{50}) is 0.023 mg/ml, comparable with the SOD activity of the cerium oxide NPs [14]. This indicates that the synthesised NPs exhibit a higher SOD activity which is the activity level of 10 U/ml biological SOD [14].

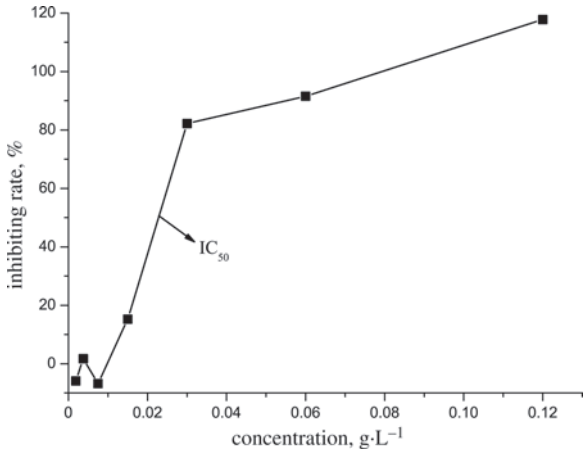

Figure 6 *Plot of the inhibition percentage against the concentration of the NPs*

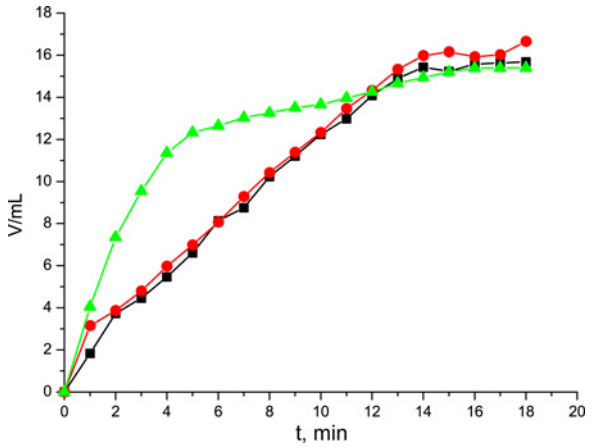

Figure 7 *H_2O_2 dismutation curve of H_2O_2 without the catalyst (a); Mn $(OAc)_2{\cdot}12H_2O$ (b) and NP (c) in 1 ml H_2O_2 (3%) aqueous solution, $T = 25°C$*

Fig. 7 shows the curve of the volume of oxygen produced by H_2O_2 in the absence and the presence of $Mn(OAc)_2{\cdot}12H_2O$ and the catalyst, respectively. The evolution profile suggests the involvement of a fast catalytic process occurring at the initial stage followed by a short slow period process, which is corresponding with the literature [16]. The initial decomposing reaction rate of H_2O_2 catalysed by the NPs was calculated as 2.69×10^{-6} mol (O_2)/s which was much higher than that of the self-dismutation of H_2O_2 or by $Mn(OAc)_2{\cdot}12H_2O$ catalysing.

4. Conclusions: In summary, silica NPs modified by imidazole, carboxyl and phenol groups were synthesised for the first time. The NPs have a spherical structure and can be easily dispersed in the reaction media because of their small size, as observed by SEM. 27% of the organic substances have been immobilised on the surface of the NPs, identified by the weight loss in the TGA and the functionalised groups in the NPs have been confirmed by the IR spectra. This kind of functionalised mimic was proven to have both higher SOD and CAT enzymatic activities. This Letter reveals that the silica NPs can be used as promising carriers for the immobilisation of multifunctionalised groups.

5. Acknowledgments: The authors acknowledge financial support from the National Natural Science Foundation of China (grant no. 21171135), China Hubei Provincial Science and Technology Department (2011BFA020), the National Center of Phosphor Resources Development and Utilization Engineering and Technology (no. k004, 2012) and the open fund of the Engineering Research Center of Nano-Geo Materials of the Ministry of Education China University of Geosciences, Wuhan (CUGNGM201311).

6 References

[1] Hu P., Tirelli N.: 'Scavenging ROS: superoxide dismutase/catalase mimetics by the use of an oxidation-sensitive nanocarrier/enzyme conjugate', *Bioconjugate Chem.*, 2012, **23**, pp. 438–449
[2] Reddy M.K., Wu L., Kou W.: 'Anuja ghorpade, vinod labhasetwar, superoxide dismutase-loaded PLGA nanoparticles protect cultured human neurons under oxidative stress', *Appl. Biochem. Biotechnol.*, 2008, **151**, pp. 565–577
[3] He W., Wu X., Liu J., *ET AL.*: 'Design of AgM bimetallic alloy nanostructures (M=Au, Pd, Pt) with tunable morphology and peroxidase-like activity', *Chem. Mater.*, 2010, **22**, pp. 2988–2994
[4] Xu J., Li Z., Xu P., Xiao L., Yang Z.: 'Nanosized copper oxide induces apoptosis through oxidative stress in podocytes', *Arch. Toxicol.*, 2012, **87**, pp. 1067–1073

doi: 10.1049/mnl.2013.0646

[5] Rosenthal R.A., Huffman K.D., Fisette L.W., *ET AL.*: 'Orally available Mn porphyrins with superoxide dismutase and catalase activities', *J. Biol. Inorg. Chem.*, 2009, **14**, pp. 979–991
[6] Chen X., Zhao T., Zou J.: 'A novel mimetic peroxidase catalyst by using magnetite-containing silica nanoparticles as carriers', *Microchim. Acta*, 2009, **164**, pp. 93–99
[7] Falahati M., Saboury A.A., Shafiee A., Ma'mani L., Moosavi-Movahedi A.A.: 'Immobilization of superoxide dismutase onto ordered mesoporous silica nanoparticles and improvement of its stability', *J. Iran. Chem. Soc.*, 2012, **9**, pp. 157–161
[8] Gu J., Xia F., Wu Y., Qu X., Yang Z., Jiang L.: 'Programmable delivery of hydrophilic drug using dually responsive hydrogel cages', *J. Control. Release*, 2007, **117**, pp. 396–402
[9] Wang Q., Wilson C., Blake A.J., Collinson S.R., Tasker P.A., Schröder M.: 'The one-pot halomethylation of 5-substituted salicylaldehydes as convenient precursors for the preparation of heteroditopic ligands for the binding of metal salts', *Tetrahedron Lett.*, 2006, **47**, pp. 8983–8987
[10] Xing Z., Wang C., Yan J., Zhang L., Li L., Zha L.: 'pH/temperature dual stimuli-responsive microcapsules with interpenetrating polymer network structure', *Colloid Polym. Sci.*, 2010, **288**, pp. 1723–1729
[11] Chung H.J., Kim H.K., Yoon J.J., Park T.G.: 'Heparin immobilized porous PLGA microspheres for angiogenic growth factor delivery', *Pharm. Res-Dordr.*, 2006, **23**, pp. 1835–1841
[12] Wang R., Hao C., Wang Y., Li S.: 'Amino acid Schiff base complex catalyst for effective oxidation of olefins with molecular oxygen', *J. Mol. Catal. A, Chem.*, 1999, **147**, pp. 173–178
[13] Singh U.P., Singh R.K., Isogai Y., Shiro Y.: 'Design and synthesis of de novo peptide for manganese binding', *Int. J. Pept. Res. Ther.*, 2006, **12**, pp. 379–385
[14] Clark A., Zhu A., Sun K., Petty H.R.: 'Cerium oxide and platinum nanoparticles protect cells from oxidant-mediated apoptosis', *J. Nanoparticle Res.*, 2011, **13**, pp. 5547–5555
[15] Yang X., Chen Q., Song J.: 'Tumor-imaging core-shell nano-models for catalase', *Chin. J. Inorg. Chem.*, 2012, **28**, pp. 164–170
[16] Gao J., Martell A.E.: 'Silica-bound dimanganese(II) complex. A robust material for heterogeneous disproportionation of H_2O_2 in aqueous solution', *Inorg. Chim. Acta*, 2003, **343**, pp. 343–346
[17] Sharma S., Sinha S., Biswas P., Maurya M.R., Chand S.: 'Oxidation of styrene over polymer- and nonpolymer-anchored Cu(II) and Mn (II) complex catalysts', *J. Appl. Polym. Sci.*, 2013, **127**, pp. 3424–3434